Nano Catalyst for CO$_2$ Conversion to Hydrocarbons

S. Tajammul Hussain[1], [2]M. Hasib-ur-Rahman[2]

ABSTRACT

A supported trimetallic nano catalyst and a fixed bed catalytic process have been developed for the conversion of CO$_2$ + H$_2$O (in the form of steam) + 1% H$_2$ to alcohol and propyne The mixture of CO$_2$ +H$_2$O and H$_2$ is passed over Ru:Mn:Ni nano catalyst dispersed on a high surface area antase titanium dioxide catalyst support at 773 K and at atmospheric pressure with the gas space velocity of 6000-7000/h. The catalytic reaction produces ethanol and propyne.

The catalyst simultaneously splits water into hydrogen and oxygen, and carbon dioxide into carbon and oxygen under very mild reaction conditions and at atmospheric pressure. The oxygen generated during the reaction not only generates considerable amount of energy for the reaction to proceed but also sustains the oxidation states of Ru, Mn and Ni, a key step in the process.

Keywords: carbon dioxide, water, hydrogen, supported catalyst, methyl alcohol, propyne

I. Introduction

Utilization of carbon dioxide (CO$_2$) has become an important global issue due to significant and continuous rise in atmospheric CO$_2$ concentration. Accelerated growth in the consumption of carbon-based energy world wide, depletion of carbon based energy resources, and low efficiency in current energy systems has created enormous interest among scientists to find viable alternative sources of sources of energy; especially ones utilizing green house gases.

The strategic objectives for CO$_2$ utilization may include:

- Use of CO$_2$ to produce industrial chemicals useful as ingredients of other products;
- Use of CO$_2$ as beneficial fluid for processing or as a medium for energy recovery and emission reduction; and
- Use of CO$_2$ recycling involving renewable sources of energy to conserve carbon resources for sustainable development.
- Use of CO$_2$ for environmentally benign physical and chemical process;

The approaches for enhancing CO$_2$ utilization may include:

- Develop effective processes for using the CO$_2$ concentrated flue gas from industrial plants or CO$_2$-rich resources without CO$_2$ separation;
- Develop more efficient and less energy intensive processes for separation of CO$_2$ selectively without the negative impacts of co-existing gases; and
- Recycle CO$_2$ as C-source for chemicals and fuels using renewable sources of energy.

In the past, several processes have been used and proposed for conversion and utilization of CO$_2$ as a source of energy [1-11]. The first process, which to date is used on an industrial scale, is the Sabatier reaction and the water gas shift reaction [12,13]. It uses hydrogen to convert CO$_2$ into alcohols and hydrocarbons, though requires both high temperature and high pressure. CO$_2$ reforming of methane over Co-Pd/alumina supported catalyst has been also used to convert the green house gas to syn gas (CO + H$_2$) and then to oxygenates. This is a two step process, which from

---

[1] National Centre for Physics, Quaid-i-Azam University, Islamabad 43520, Pakistan. Corresponding author: dr_tajammul@yahoo.ca , Ph: +00-92-51-2077308, Fax: +00-92-51-2077395
[2] Department of Chemistry, Quaid-i-Azam University, Islamabad, 45320, Pakistan

the economics point of view, is not very attractive for the industries [14]. The main drawback in these processes presently at industrial scale is the utilization of extra energy in the form of hydrogen, which at industrial level is obtained by decomposition of natural gas or electrolysis of water and the use of higher temperature and higher pressure. This makes the whole technology economically unfeasible for industries.

The catalytic process for the utilization of CO_2 developed in our laboratory will be a step towards the development of technology for alternate energy production and environmental control. In this process, a multimetallic supported nano catalyst has been developed with specific surface/bulk oxide geometry and controlled interaction with the support. Water in the form of steam and carbon dioxide decomposes over the catalyst surface to produce oxygen and hydrogen. The hydrogen and oxygen reacts *in situ* with carbon to produce ethanol and propyne according to the following graphical abstract, Figure 1 and Equation 1.
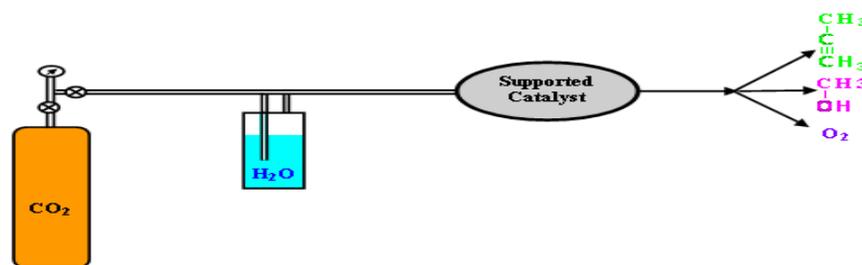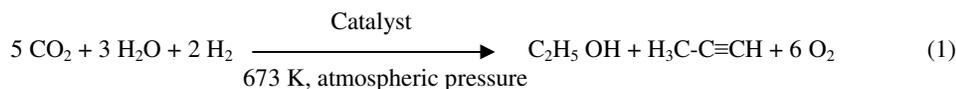

Figure 1. Graphical abstract of the process

$$5 \: CO_2 + 3 \: H_2O + 2 \: H_2 \xrightarrow[\text{673 K, atmospheric pressure}]{\text{Catalyst}} C_2H_5 \: OH + H_3C\text{-}C{\equiv}CH + 6 \: O_2 \quad\quad (1)$$

The introduction of 1% hydrogen into the catalytic reactor helps to maintain the oxidation states of the Ru, Mn, Ni which are necessary active catalytic sites for the reaction to proceed. Otherwise the oxygen generated from water splitting changes the Ru, Mn and Ni to different oxidation states, thus the product formation is inhibited and the catalyst deactivates.

On the other hand, environmental problems due to excessive emission of green house gas that cause global climate change will be overcome with the use of this new technology. According to recently published reports [15,16,17], if this problem of global warming could not be solved in the near future, up to 40% of species will become extinct by the end of 21st century. This investigation is a step towards the development of a renewable source of energy and control over the emission of green house gas.

II. Experimental Methods

A. Preparation of supported catalyst

A solution of ruthenium trichloride (0.103 g), manganese nitrate tetrahydrate (2.285 g) and nickel nitrate hexahydrate (2.47 g) (analar grade BDH Chemicals Ltd) in deionized water, acidified with dilute hydrochloric acid to prevent the precipitation of hydroxide was prepared. A portion of the slurry (10 cm^3) was added to the titanium dioxide catalyst support (3.95 g), (350 m^2g^{-1}) catalyst support in an evaporation basin and the mixture was magnetically stirred. The slurry was stirred for 20 minutes and dried at 395 K overnight. The prepared catalyst sample was calcined in air for 6 hours at 600 °C. Different loadings of Ru, Mn and Co ranging from 2-3% Ru, 20-30% Ni, 15-20% Mn were prepared and subjected to catalytic testing. The sample with 2% Ru, 20%Ni, 15%Mn was found to be best, and finally selected for further characterization and catalytic testing. The sample was designated as SM-1.

B. Characterization of Catalysts

A Scanning Electron Microscopy (SEM) image and backscattering electron images of the catalyst were characterized using a Hitachi FE-SEM S-800 (field emission gun scanning electron microscopy) and Phillips TEM Model No. SS-5412

X-ray diffraction pattern were characterized by a Rigaku RINT 2500 V diffractometer using Cu-Kα radiation at room temperature operated at 40 kV and 100 Amp.

The surface concentration of ruthenium, manganese and potassium were determined with static secondary ion mass spectrometry (SSIMS). The positive secondary ion generated on bombardment of the surface of the catalysts with an argon ion beam were analyzed using a VG 12-12 quadrupole mass spectrometer. The incident argon ions had an energy of 2 KeV; a current of 1 nA/cm^2 was used.

X-ray photoelectron spectra (XPS) were recorded in a VG ESCA-III instrument using Mg-Kα radiation. Targets were prepared from powder samples. Prior to analysis, the samples were sputtered with an argon ion beam with an ion current of 20 µA for 5 seconds to remove hydrocarbons adsorbed on the surface. Binding Energies (BE) of all the elements were calculated using 284 eV C1s BE peak as standard.

C. Characterization of Catalyst Using SEM/TEM

The surface morphology and geometry of the catalytic active sites and their interaction with the support was studied by SEM and the result is presented in Figure 2 and TEM results in figure 3. Table 1 presents the EDX analysis showing the percentage composition of metals dispersed inside the pore of titanium dioxide support.
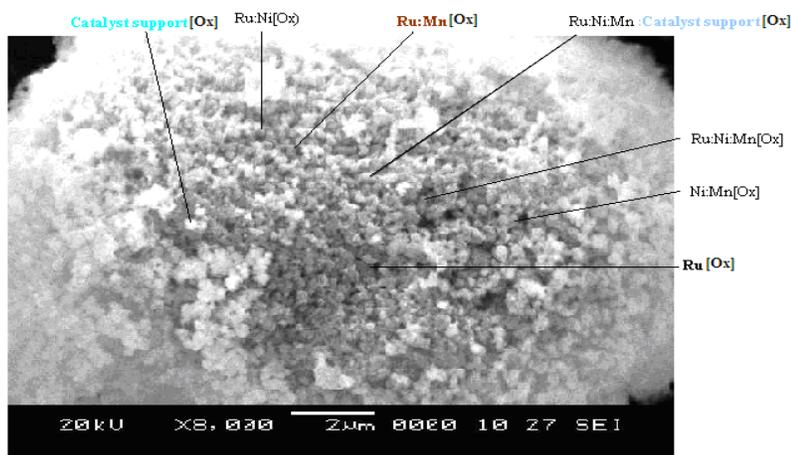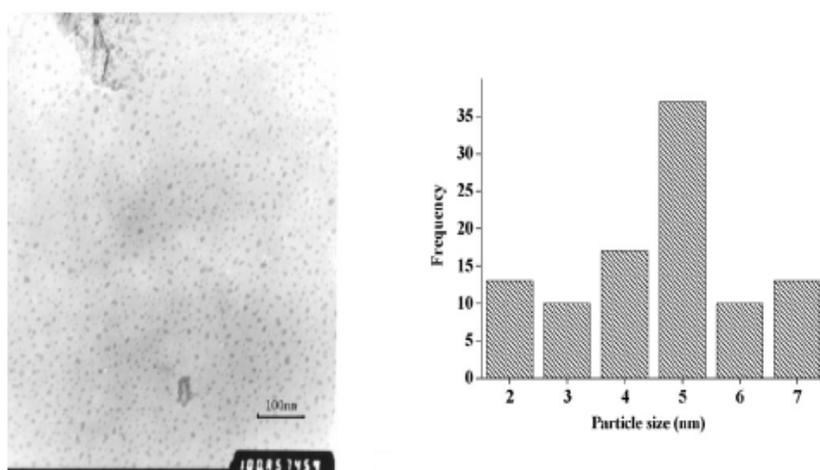

Figure 2. SEM view of the catalyst surface.

Figure 3. TEM study of the Catalyst system.

Table 1. EDX analysis of SEM view presented in Figure 1.

Catalyst (TM-1)	Ru (%)	Mn (%)	Ni (%)	Ti (%)	O (%)
SM-1	1.90	13.2	21.01	39.78	24.02

D. Characterization of Catalyst Using XRD (X-ray diffraction)

The results of XRD analysis of SM-1 catalyst are presented in Figure 4. About 0.5 g. of the powder sample was pressed into glass window backed by a glass slide and smoothed to an even packing with a spatula. The sample was mounted into a diffraction chamber, and scanned from Bragg angle $2\theta = 16°$ to $2\theta = 70°$. The peak identification was accomplished through comparison of measured spectra with ASTM (American Society for Testing Materials) powder data file. The particle size calculated from XRD data using Scherrer equation came out to be 5 nm.
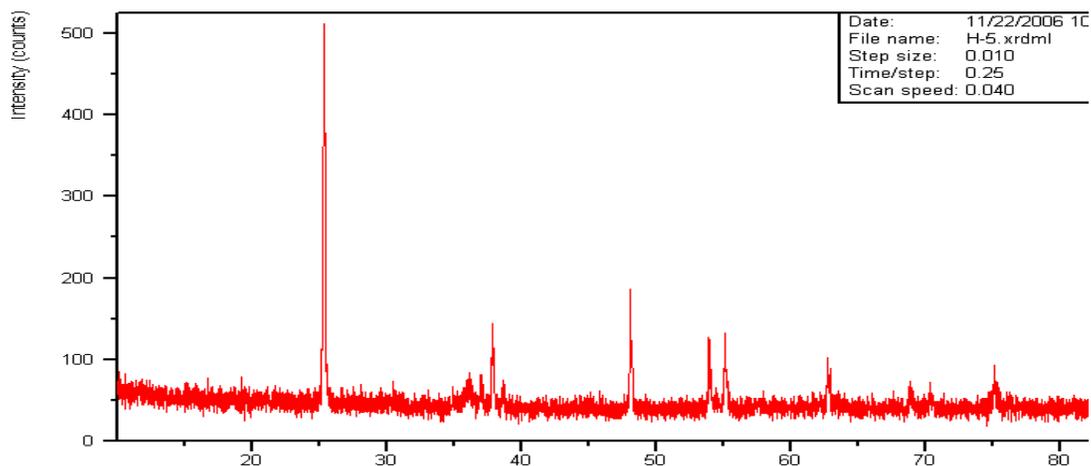

Figure 4. XRD analysis of SM-1 catalyst.

E. Characterization of Catalyst using SSIMS

Table 2 presents the secondary ions analysis of the SSIMS spectra, which clearly indicates the interaction of Ru, Mn, and Ni (Ox) creating a trimetallic surface geometry. An interaction of with Ru:Ni:Mn (Ox) with titanium dioxide is observed.

Table2. SSIMS analysis.

Amu	Peak Identification
118	RuO
142	MnO_2
166	Ni_2O_3
189	$RuMnO_2$
247	$MnONi_2O_3$
332	$Ni_2O_3RuO_4$
645	$RuOMnO_2Ti_2O_3$

F. Characterization of Catalyst Using XPS

The XPS analysis of SM-1 for C_{1S} and O_{1S} region were performed and the results are presented in Figure 5. It can be seen that carbon produced from the decomposition of CO_2 transforms in C1, C2 and C3 type carbon species on the surface of the catalyst and from decomposition of water in to two types of oxygen O1 and O2.
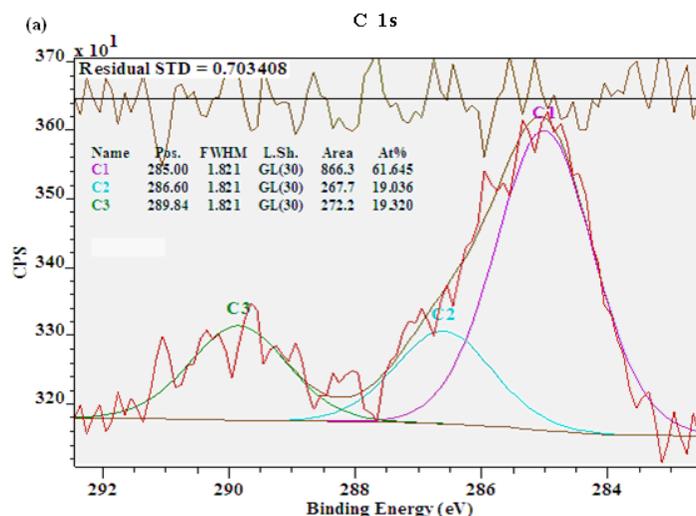

Figure 5. XPS spectrum of the spent catalyst showing C_{1S} and O_{1S} formation on the surface.
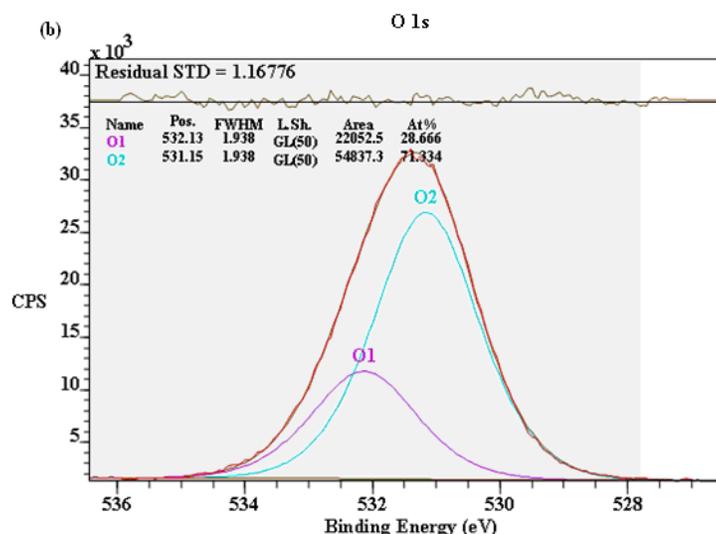

Figure 6. The BET analysis of SM-1 catalyst.

H. Catalytic Studies

The catalytic test was carried out in the fixed bed catalytic reactor system (see Figure 6). The catalyst loading of 0.5 g was placed inside the catalytic reactor tube. Quartz wool at both ends and the titanium dioxde support was used to hold the catalyst. The catalyst bed was heated with argon at the reaction temperature of 673 K for 2 h to remove any surface impurities. The argon is then replaced with reactant mixtures (CO_2+Steam+H_2). The out let of the product

steam is connected to the on line GC/MS [Gas Chromatography/Mass Spectrometry] for product analysis. The product selectivity and the conversion was calculated by the inbuilt software. The unreacted mixture of product streams is re-circulated over the catalyst bed.
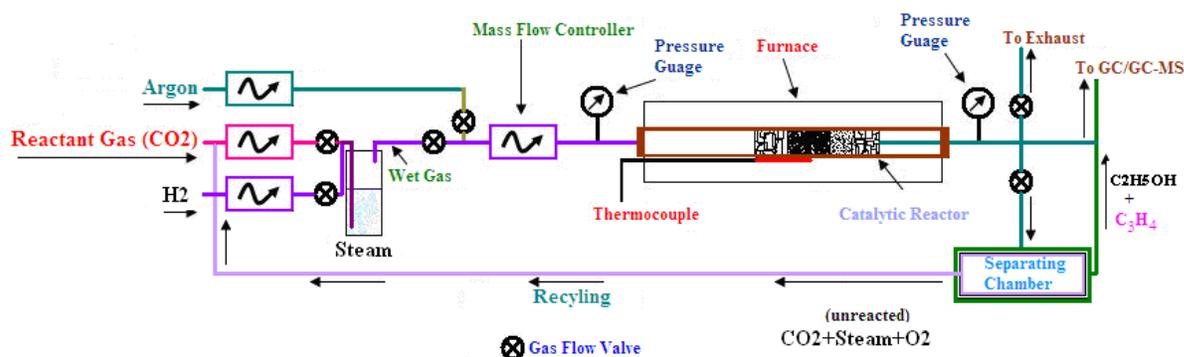

Figure 6. The design of carbgas (CO₂ + H₂O) conversion process into oxygen, ethanol, and propyne.

III. Results and Discussion

The catalyst activity test was performed using the newly developed catalytic process presented in Figure 7. Carbgas, steam and 1% hydrogen with the space velocity in between 6000-7200/h is passed over the catalyst surface in a fixed bed reactor, at 773 K. During the catalytic process, C-O and H-OH bonds break forming CH_x surface intermediate. This intermediate combines with OH to produce ethanol and propyne in a series of steps as discussed in proposed mechanism presented in Figure . The nacent oxygen produced from splitting of H-O-H bonds results in the generation of extra amount of energy, since the reaction becomes autothermal, minimizing the external energy requirement to heat the system.. The analysis of the product stream was performed by online GC/MS (Gas Chromatography/Mass Spectrometry) and FTIR (Fourrier Transform Infrared Spectroscopy). The results are presented in Table 3 and Table 4, respectively.

Table 3. MS analysis of the product stream.

Catalyst Designation	%Ethyl Alcohol Production At 3 50/400/450 0C (amu 32)	%age Propyne Production At 3 50/400/450 0C (amu 40)	Time (Hrs)
SM-1	8/13/15	12.5/17/20	0.5
	11/15/19	19/25/28	1.0
	14/19/23	22/30/32	1.5
	18/22/26	27/30/37	2.0
	19/24/36	30/36/41	3.0

<center>**Table 4. FTIR analysis of the product stream.**</center>

Catalyst Designation	MS analysis (m/z)	FTIR analysis (cm^{-1})
SM-1	40 (Propyne)	2072 (C≡C)
	46 (C_2H_5OH)	3595 (OH)

A MTI (Microsensor Technology Inc.) dual-module micro gas chromatograph (MTI 200H) with a TCD detector was used to analyze the gaseous products and ethanol as well as water using Poraplot Q column and a molecular sieve column. This GC was coupled with Balzer 5100 Mass Spectrometer. GC data was used to calculate the mass balance and selectivity, and MS data was used to calculate the percentage composition of each product constituents. All results are reported in mole percent. The mass balance of the reaction was obtained by adding a controlled flow of nitrogen as reference gas to the exit of the reactor in order to monitor the change in volume of the reaction.

The conversion of CO_2 is defined as:

Conversion [reactants]$_i$ = [reactants)$_{i(in)}$ –[reactants]$_{i(out)}$/[reactants]$_{i(in)}$} x 100%

The yield of the product is defined as:

Yield [mol%]$_i$ = [products]$_i$/[(O_2)$_{in}$ + [H_2O]$_{in}$ + [O_2]$_{in}$

The selectivity of the products is calculated as:

Selectivity [product]$_i$ = [(number of carbon]x [product]$_i$] /[carbon number converted] x 100%

The data presented in Table 1 show that the percentage selectivity of ethanol and propyne increases as the reaction proceeds. After 3 hours of the reaction the production of ethanol (amu 46) and propyne (amu 40) reaches 19% and 30%, respectively. The products were further confirmed from the *in situ* FTIR studies presented in Table 4, which show broad absorption at 3595 cm^{-1} due to OH bond and steep signal at 2072 cm^{-1} due to C≡C bond.

A. The Reaction Mechanism

The XPS analysis suggests the formation of different types of carbon and oxygen (sub and molecular oxygen) during the catalytic run. This, we believe, acts as a chain propagation initiator for the production of alcohol and propyne intermediate.

The hydrogen generated from the splitting of water and 1% hydrogen addition results in the creation of specific oxidation states of the Ru, Mn, and Ni. These oxidation states are the key catalytic sites, which are regenerated during the catalytic studies. These oxidation sites of Ru, Mn, and Ni generate the intermediates by breaking O-C-O bonds and formation of the C-H$_x$ intermediate (see Figure 7).
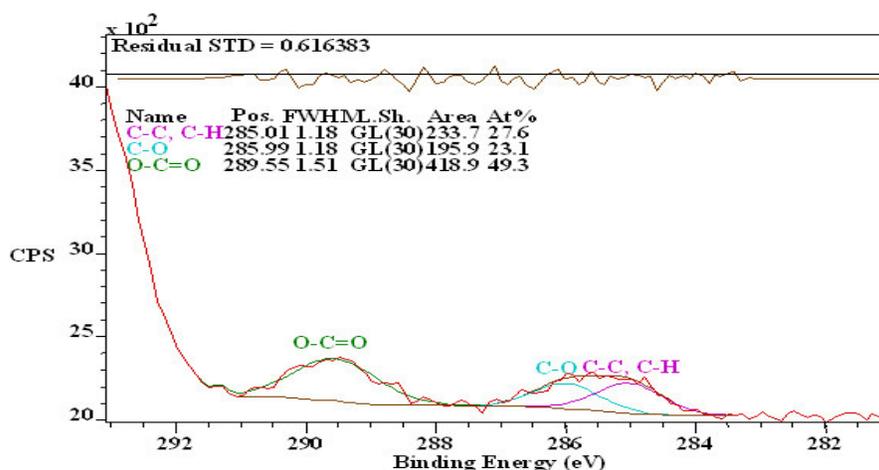

Figure 7. XPS study of the SM-1 catalyst system during catalytic reaction indicating the formation of chain growth.

These species are responsible for the production of alcohol and propylene. The generated oxygen from water splitting during the catalytic run directs the reaction towards auto thermal mode and contributes significantly towards the retention specific oxidation geometry of the catalyst system.

Based on our catalyst product analysis by MS, FTIR, XRD, and XPS a mechanism of the product formation is proposed and presented in figure 8.
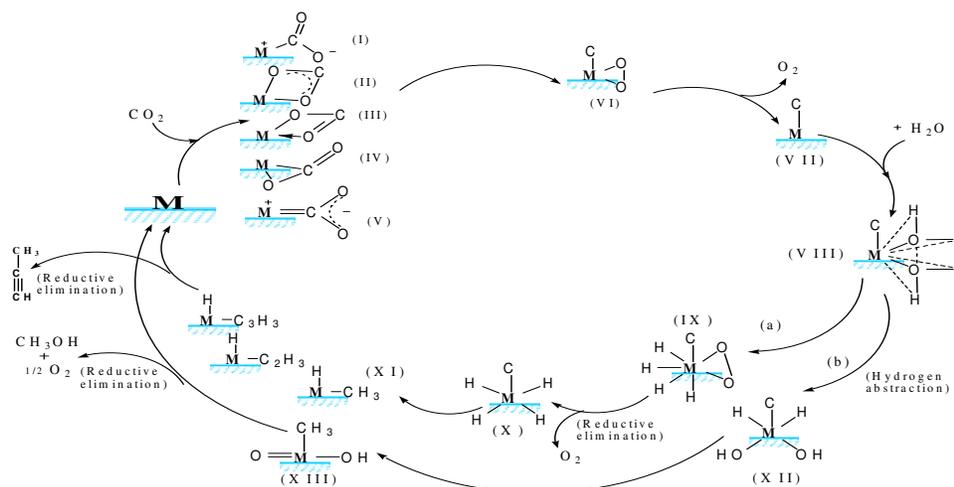

Figure 8.. The interaction of different metals species and their role for the product formation.

The postulated mechanism depicts that accumulated electrons in the support during the reaction are transferred into the lattice of Ru/Co to promote activation of CO_2 on the surface by polarizing linear CO_2 to bent CO_2 molecule to interact with the catalyst active sites to give complex (I). The complex (I) rearranges itself to give species (II), (III), (IV), and (V) etc.

Species (II) and (III) abstract oxygen by cleavage of two O-C bonds and formation of O-O bond to give species (VI), which on reductive elimination of O_2 gives species (VII). This is the key step in carbon dioxide activation and decomposition. Species (IV) and (V) do not seem to be present in sizable amount as formation of formic acid or formaldehyde was not detected in the product stream. However, presence of these species cannot be ruled out altogether; further study is planned to confirm the hypothesis. Newly formed species (VII) with M-C bond react with surface adsorbed HOH to give species (VIII). Here splitting of H_2O takes place via two steps (a) and (b). Step (a) leads to decomposition of water by abstracting oxygen to form a complex containing molecular oxygen and metal hydride. Reductive elimination of O_2 and insertion of carbon into M-H bond leads to successive formation of H-M-CH_3, H-M-C-CH_3 and H-MC-C-CH_3. Finally, through a reductive elimination step, propyne is eliminated, and catalyst is regenerated for recycling. Accumulation of electrons in the n-type semi conducting solid support is enhanced by the presence of high valent manganese ions present as trimetallic catalyst site represented as M in figure 12. In route (b) water adsorbed on the surface of the species (VII) oxidatively adds to metal to give hydride and hydroxo complex to yield species (XIII) which on reductive elimination produces C_2H_5OH and O_2 regenerated for taking the reaction in an auto-thermal mode. Water adsorbed on the surface of the catalyst, most likely Ru, in bilayers gets partially dissociated with one OH bond broken as has been previously reported [16].

IV. Conclusions

* A new catalytic material and catalytic process has been deveolped having controlled surface species responsible for the catalytic reaction.

* The carbgas ($CO_2 + H_2O + H_2$) is converted to ethyl alcohol and propyne at 773 K and at atmospheric pressure.

* The presence of different oxidation states of trimetallic supported catalyst system breaks H-OH and C-O bonds simultaneously, producing carbon and oxygen.

* The presence of specific oxidation geometry of Ru, Mn, Ni, and TiO_2 is the key to the catalytic reaction.

* The metal's (Ru, Mn, Ni[O_x], TiO_2) support interaction results in an increase in catalyst active sites and contributes towards the stability of the system.

* The role of TiO_2 in enhancing the breakage of H-O-H bonds is evident due to its anatase nature and possibly a band gap of < 3.0 (eV).

* The concentration of hydrogen accumulated during the reaction contributes significantly towards the favorable thermodynamics of the reaction.

* The oxygen presence shifts the reaction in an autothermal mode.

* The reaction proceeds in a stoichiometric mode, restricting the reduction of Ru, Mn, and Ni that enables the product formation.

Acknowledgments

References

[1] K. Sayama and H. Arakawa, Photocatalytic decomposition of water and photocatalytic reduction of carbon dioxide over zirconia catalyst, J. Phys. Chem. 97, 1993, pp. 531-535.

[2] D. Mahajan, C. Song, and A.W. Scaroni, Micro-reactor study on catalytic reduction of CO_2 into liquid fuels: simulating reactions under geologic formation conditions, Am. Chem. Soc. Div. Petrol. Chem. Prepr. 45, 2000, pp. 79-81.

[3] K. Zhag, U. Kogelschatz, and B. Eliasson, Conversion of greenhouse gases to synthesis gas and higher hydrocarbons, Energy & Fuel. 15, 2001, pp. 395-401.

[4] H.J. Herzog, Using Carbon capture and sequestration technologies to address the climate change, Am. Chem. Soc. Div. Fuel Chem. Prepr. 46, 2001, pp. 53-55.

[5] H.J. Herzog, Effect of dopnat on the catalytic properties of Ce:Mn bimetallic catalyst, Environ. Sci. Technol. 35, 2001, pp. A148-153.

[6] C.S. Song, A.M. Gaffney and K. Fujimoto (eds.), *CO_2 conversion and utilization.* American Chemical Society, Washington, DC, ACS Symposium Series 809, 2002, pp. 39-47, Chapter 3.

[7] H.H. Schobert, and C.S. Song, Chemicals and materials from coal in the 21st century, Fuel, 81, 2002, pp. 15-20.

[8] C.S. Song, A.M. Gaffney, and K. Fujimoto (eds), CO_2 conversion and utilization. Edited by American Chemical Society, Washington, DC, ACS Symposium Series, 809, 2002, pp. 112-116.

[9] T. Inui and T. Yamamoto, Effective synthesis of ethanol from CO_2 on polyfunctional composite catalysts. Catal. Today 45, 1998, pp. 209-213.

[10] P.B. Weisz. Basic choices and constraints on long-term energy supplies. Phys. Today 57, 2004, pp.47-52.

[11] H. Tominaga and M. Nagai. Density functional study of carbon dioxide hydrogenation on molybdenum carbide and metal. App. Catal. A *Gen* 285, 2005, pp. 5-9.

[12] X-M, Liu, L-Z-F, Yan, and I. Beltramini. "Recent advances in catalysts for methanol synthesis via hydrogenation of CO and CO_2" J. Ind. Eng. Chem. Res.42, 2003, pp. 6518-6525.

[13] T. Matsuo and H. Kawaguchi. *J. Am. Chem. Soc.* "From carbon dioxide to methane: homogeneous reduction of carbon dioxide with hydrosilanes catalyzed by zirconium-borane complexes", 2006, 128, 12362.

[14] S.S. Itkulova, K.Z. Zhunsova, and G.D. Zakumbaeva, "CO2 reforming of methane over CO-Pd/Al_2O_3 catalysts" Bull. Korean Chem. Soc. 26, 2005, pp. 2017-2022.

[15] B. Hileman, Surfcae studies of interaction of CO_2 on metal surfaces. Chem. Eng. News. 84, 2006, pp. 7-12.

[16] S. Meng, L.F. Xu, E.G. Wang, and S. Gao, Vibrational recognition of hydrogen-bonded water networks on a metal surface" Phy. Rev. Lett. 89, 2002, pp. 1761-1767.

[17] M.H. Schmidt, G.M. Miskelly, and N.S. Lewis, Effects of redox potential, steric configuration, solvent, and alkali metal cations on the binding of carbon dioxide to cobalt(I) and nickel(I) macrocycles. J. Am. Chem. Soc. 112, 1990, pp. 34203426.